JOURNAL OF MATERIALS SCIENCE 16 (1981) 457–464

# Effect of phase proportions on deformation and cavitation of superplastic α/β brass

J. W. D. PATTERSON, N. RIDLEY
*Joint University of Manchester/UMIST Department of Metallurgy, Grosvenor Street, Manchester, UK*

Studies have been made, using metallographic and precision density techniques, of the deformation and cavitation behaviour during superplastic tensile straining at 873 K of three microduplex $\alpha/\beta$ brasses which, as a consequence of varying composition, contained varying proportions of $\alpha$ and $\beta$ phases. It was observed that both strain-rate sensitivity and elongation-to-failure passed through a maximum when approximately equivolume proportions of the two phases were present. Cavitation, on the other hand, decreased rapidly as the volume fraction of $\beta$ phase was increased. The cavitation behaviour was attributed to the relative abilities of the phases to accommodate grain boundary sliding. When a high proportion of $\alpha$ phase is present accommodation is minimal and cavity nucleation occurs readily. Evidence is presented to show that grain-boundary sliding plays a predominant role in cavity growth. When a high proportion of $\beta$ phase is present accommodation is almost complete and cavity nucleation is minimal.

## 1. Introduction

Copper-base alloys including brasses [1–3], aluminium bronzes [4] and nickel-silvers [5, 6], appear to be particularly prone to cavitation during superplastic tensile flow, and this could clearly inhibit their use in superplastic forming processes. Hence, it is important to understand the factors which influence cavitation in these systems in order to develop procedures to minimize their occurrence. For a microduplex $\alpha/\beta$ brass containing nominally 40 wt % Zn, it has been shown that the level of cavitation for a constant strain increases as stress, strain rate and grain size are increased, and decreases as the deformation temperature is increased [3].

Preliminary studies have also indicated that the level of cavitation is markedly dependent on composition [7]. The present work describes a more detailed study of the deformation and cavitation behaviour during superplastic tensile straining of three binary $\alpha/\beta$ brasses which, as a consequence of varying composition, contain varying proportions of the $\alpha$ and $\beta$ phases.

## 2. Experimental procedure

### 2.1. Materials

The $\alpha/\beta$ brasses examined contained nominally 40, 41 and 42 wt % Zn, respectively, the chemically analysed compositions are listed in Table I. The materials were supplied by IMI Ltd., in the form of 12.5 mm diameter rods which had been hot extruded at 500° C to give the required microduplex structure.

### 2.2. Tensile straining

Hounsfield type tensile specimens of gauge length 10 mm and gauge diameter 5 mm were machined from the rods. Tensile straining was carried out in air in a high temperature rig attached to an Instron tensile testing machine. The deformation temperature was 873 K since previous work had shown that this represented an optimum temperature for superplastic flow in $\alpha/\beta$ brasses [1, 3].

The materials were characterized by the strain-rate change technique developed by Backofen *et al.* [8]. The resulting relationships between flow

TABLE I Compositions and microstructural features of the brasses

| Nominal composition (wt %) | | Analysed composition | | | Vol % of $\beta$ phase at 873 K | Initial grain size (m.l.i.) ($\mu$m) |
|---|---|---|---|---|---|---|
| Present work | Previous work [7] | Cu | Fe | Zn | | |
| 60% Cu–40% Zn | – | 60.33 | ~ 0.009 | * balance | 28.4 | 8.5 |
| – | 60% Cu–40% Zn | 58.83 | 0.001 | * balance | 40.2 | 7.4 |
| 59% Cu–41% Zn | – | 58.67 | ~ 0.012 | * balance | 42.1 | 8.3 |
| – | 59% Cu–41% Zn | 58.37 | 0.04 | * balance | 47.0 | 7.6 |
| – | 58% Cu–42% Zn | 57.70 | 0.01 | * balance | 61.3 | 10.7 |
| 58% Cu–42% Zn | – | 57.12 | ~ 0.01 | * balance | 67.6 | 11.2 |

*Other elements, Pb < 0.003%, Sn < 0.005%, Ni ~ 0.01%, Mn < 0.005%, Al ~ 0.005%, Sb < 0.002%, Bi < 0.001%, As < 0.002%, Si < 0.005%.

stress and strain rate were plotted logarithmically, with the maximum gradient of the curve being used to describe the strain rate sensitivity of flow stress, $m$, for the materials.

A further comparison of the brasses was obtained by deforming specimens to failure at constant cross-head velocities corresponding to various initial strain rates in the region of maximum strain rate sensitivity.

### 2.3. Metallography and densitometry

Metallographic features of deformed specimens were examined using optical and scanning electron microscopy. For cavitated specimens final polishing was carried out using a fine grade alumina slurry to avoid tearing of cavities. Most specimens were ion-beam etched at a pressure of $10^{-1}$ mm Hg and a discharge current of ~ 19 mA for 10 to 15 min, to avoid pitting and preferential attack on the cavities often associated with conventional etching procedures. However, for comparison purposes a few cavitated specimens were etched in acid ferric chloride as were all non-cavitated specimens. Grain size measurements were made using the mean linear intercept (m.l.i.) method. The volume fractions of $\alpha$ and $\beta$ phases present in each alloy, after quenching from the deformation temperature of 873 K, were determined with a Swift semi-automatic point counter.

To determine overall levels of cavitation, density measurements were made on the gauge lengths of specimens deformed to predetermined extents at various initial strain rates. The measurements were made by hydrostatic weighing in ethyl iodide contained in a Dewar flask, with the undeformed heads of tensile specimens being used as density standards.

## 3. Results

### 3.1. Mechanical behaviour

Stress–strain rate relationships for the three alloys at 873 K are plotted logarithmically in Fig. 1 for strain rates in the range $1.67 \times 10^{-3}$ to $8.3 \times 10^{-5}$ $sec^{-1}$, as an earlier study had shown that maximum superplastic response was likely to lie in this range [3]. The maximum value of strain rate sensitivity of flow stress for each alloy and the corresponding strain rate range is included in Table II. It can be seen from Fig. 1 that at higher strain rates the flow stress decreases with increasing zinc content, although at lower rates the flow stress for the 42% Zn alloy becomes higher than that for the 41% Zn alloy.

Results of constant cross-head velocity to failure tests are included in Table II. The elongations obtained for a range of strain rates tended to be greater for the 41% Zn alloy than those measured for the other two alloys, with the values obtained for the 40% Zn alloy being appreciably smaller than those recorded previously [3, 7] for a material of nominally similar composition.

### 3.2. Density studies

Density measurements were made on the three brasses to determine the overall level of cavitation at 873 K for specimens deformed at initial strain rates within the range $10^{-3}$ to $10^{-4}$ $sec^{-1}$. Fig. 2 shows the variation of the volume of cavities with

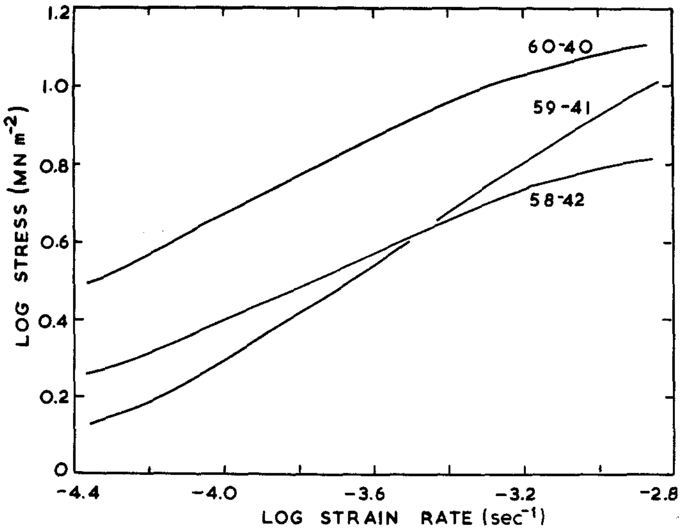


*Figure 1* Logarithmic plot of flow stress against strain rate at 873 K for the three $\alpha/\beta$ brasses.

elongation for specimens deformed at an initial strain rate of $3.33 \times 10^{-4}$ sec$^{-1}$. It can be seen that the 40% Zn alloy cavitates very rapidly with increasing strain, whereas the 42% Zn alloy shows only slight cavitation; the behaviour of the 41% Zn alloy lies between these two extremes.

Fig. 3 shows the variation of cavitation with strain rate for each material for a constant elongation. For the 40% Zn alloy the level of cavitation is relatively constant for strain rates up to $8.3 \times 10^{-4}$ sec$^{-1}$, and falls slightly thereafter. For the 41% Zn alloy the level of cavitation increases slowly with increasing strain rate, while for the 42% Zn alloy cavitation is essentially constant at a low level.

### 3.3. Metallography

An important microstructural feature of deformed specimens containing 40% Zn and 41% Zn was the presence of cavities along the whole of the gauge length while the 42% Zn alloy showed only slight cavitation, with most of the cavities in specimens pulled to failure being located in the vicinity of the fracture surfaces. Fig. 4 shows cavity distribution near the fracture faces for the three alloys pulled to failure at a constant cross-head velocity of $3.33 \times 10^{-3}$ mm sec$^{-1}$. These specimens were etched in acid ferric chloride solution.

The relative numbers of cavities in different types of sites in the 3 alloys was examined for specimens elongated to various extents from a range of initial strain rates. Typical results are shown graphically in Fig. 5 for specimens deformed at an initial strain rate of $3.33 \times 10^{-4}$ sec$^{-1}$.

Scanning electron microscopy studies of the fracture surfaces showed that although impurity particles were sometimes associated with cavities, this was by no means a common occurrence.

## 4. Discussion

### 4.1. Strain rate sensitivity and elongation to failure

The sigmoidal shapes of the logarithmic stress–strain rate curves shown in Fig. 1 have been frequently reported for microduplex alloys. At the higher strain rates, where dislocations are likely to play an increasingly significant role in the deformation process, the stress levels decrease with increasing zinc content, i.e. increasing volume fraction of $\beta$ phase. This observation is consistent with

TABLE II Deformation characteristics of the brasses

| Nominal composition (wt %) | Maximum $m$ | Approximate strain rate range, ($\times 10^4$ sec$^{-1}$) | Maximum tensile elongation (%) |
|---|---|---|---|
| 60% Cu–40% Zn | 0.52 | 0.5–3 | 171 |
| 59% Cu–41% Zn | 0.65 | 1–8 | 410 |
| 58% Cu–42% Zn | 0.43 | 0.8–6 | 277 |

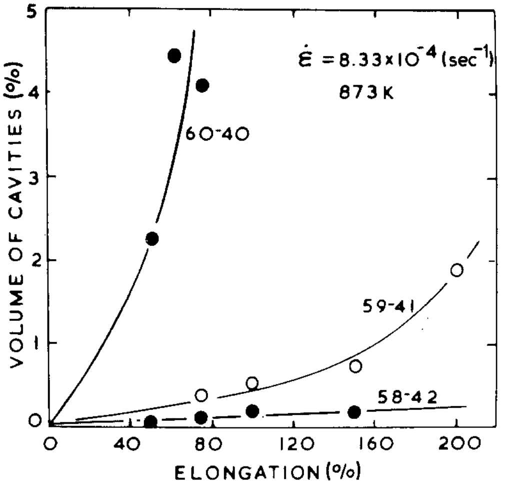


*Figure 2* Volume of cavities as a function of tensile elongation at 873 K. Initial strain rate $3.33 \times 10^{-4}$ sec$^{-1}$.

the well-known fact that during hot-working, $\beta$ brass is much more readily deformed than $\alpha$ brass. As the strain rate is decreased the flow stress for the 42% Zn alloy becomes greater than that for the 41% Zn alloy. It is likely that this effect is due to the lower strain rate sensitivity of flow stress of the former alloy, which contains a high proportion of $\beta$ phase, and to its larger grain size which would lead to an increase in flow stress. (Table I). It is also apparent from Fig. 4 that the 42% Zn alloy is particularly prone to grain growth during deformation.

Table II gives some deformation characteristics of the 3 brasses, and it can be seen that the 41% Zn alloy exhibits both the highest "$m$" value and the highest maximum-elongation-to-failure. This behaviour can be related to the volume proportions of the two phases in the alloy, which are approximately equal. The observation is in accordance with the earlier proposals attributable to Crane (as discussed in [9]), who suggested that, for a microduplex aluminium bronze, the proportions of the $\alpha$ and $\beta$ phases were important in controlling the superplastic tensile ductility. Taplin and Chandra [9] have reported that maximum tensile elongations in microduplex copper alloys are obtained when equal proportions of $\alpha$ and $\beta$ phases are present, and they also observed a decreasing flow stress with increasing proportion of $\beta$ phase.

In comparison, the 40% Zn alloy gave consistently lower elongation-to-failure values than the 42% Zn alloy despite the fact that the latter had a smaller maximum $m$ value, i.e. 0.43 compared to 0.52. This behaviour can be accounted for in terms of the differences in cavitation behaviour between the two alloys, and will be discussed in the next section.

## 4.2. Cavitation behaviour

If, during superplastic flow, the rate of sliding at a point on a boundary exceeds the rate of accommodation, by diffusional or dislocation processes, then the resulting stress will lead to cavity nucleation. Hence, the formation of cavities at potential nucleating sites on a grain or phase boundary will reflect the extent to which the boundary is involved in the sliding process and also the ability of the phases adjoining the boundary to accommodate the sliding. For $\alpha/\beta$ brasses, therefore, it should be possible to relate cavitation behaviour to the ease with which $\alpha/\alpha$, $\alpha/\beta$ and $\beta/\beta$ boundaries can slide and to the contributions which the $\alpha$ and $\beta$ phases can make to the accommodation processes. The relative volumes of $\alpha$ and $\beta$ phases

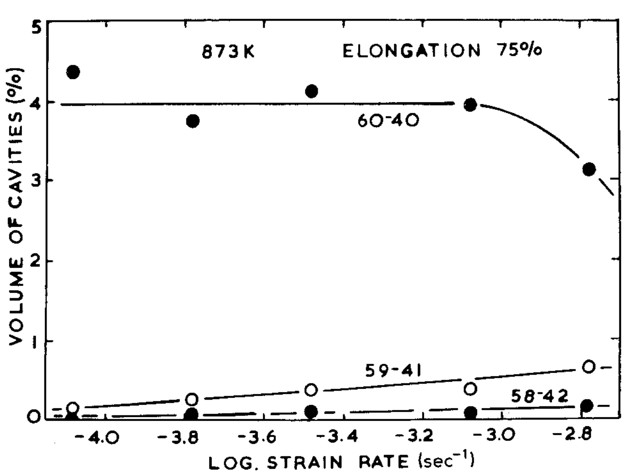


*Figure 3* Volume of cavities as a function of initial strain rate for a constant elongation of 75% at 873 K.

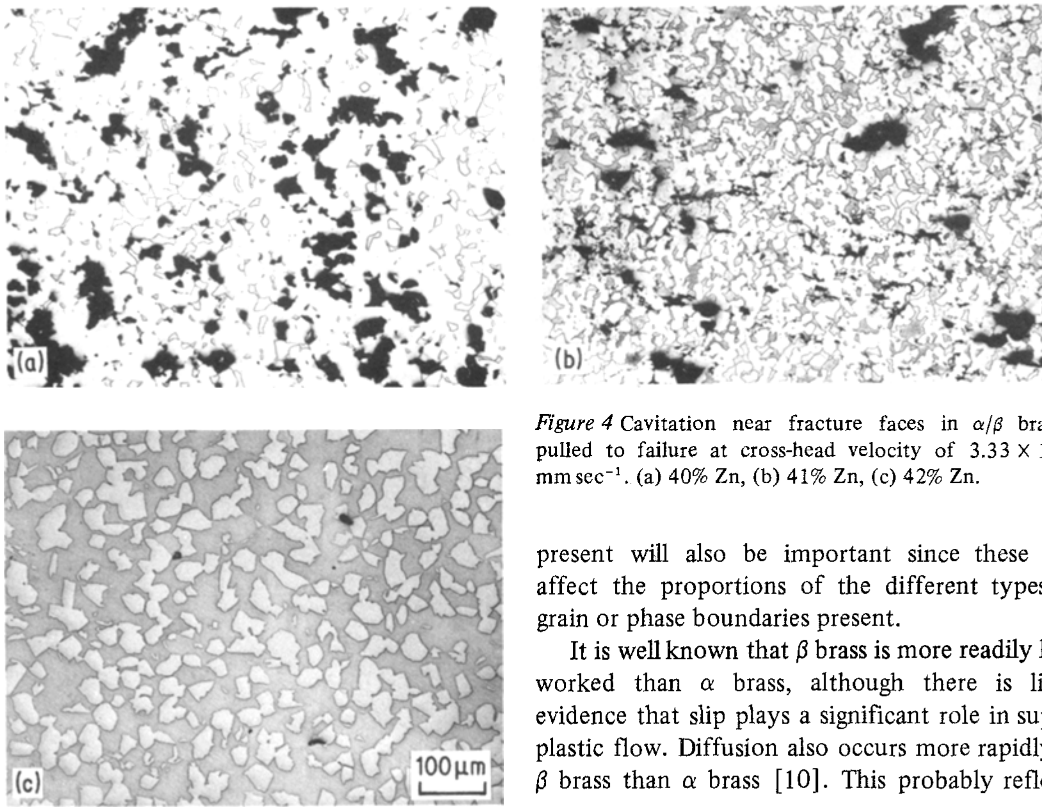


*Figure 4* Cavitation near fracture faces in $\alpha/\beta$ brasses pulled to failure at cross-head velocity of $3.33 \times 10^{-3}$ mm sec$^{-1}$. (a) 40% Zn, (b) 41% Zn, (c) 42% Zn.

present will also be important since these will affect the proportions of the different types of grain or phase boundaries present.

It is well known that $\beta$ brass is more readily hot-worked than $\alpha$ brass, although there is little evidence that slip plays a significant role in superplastic flow. Diffusion also occurs more rapidly in $\beta$ brass than $\alpha$ brass [10]. This probably reflects

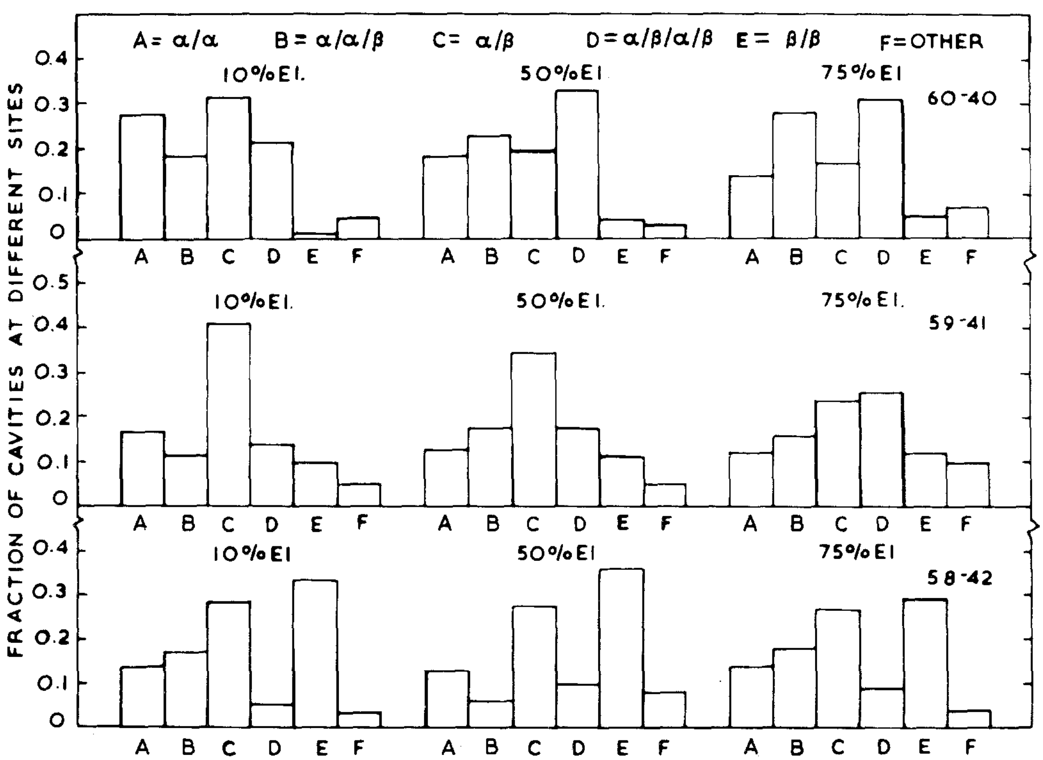


*Figure 5* Relative numbers of cavities at different sites as a function of strain at 873 K. Initial strain rate $3.33 \times 10^{-4}$ sec$^{-1}$. El = elongation.

the less closely-packed structure of the b c c phase and the fact that, for a given temperature, the $\beta$ phase in an $\alpha/\beta$ brass is at a higher homologous temperature than the co-existing $\alpha$ phase.

Chandra *et al.* [2] have studied an $\alpha/\beta$ brass containing approximately equal volume proportions of the two phases, and have found that at 873 K the sliding rate at $\alpha/\beta$ interfaces is about $1\frac{1}{2}$ times that at $\alpha/\alpha$ boundaries and $2\frac{1}{2}$ times that at $\beta/\beta$ boundaries. The relative ease of sliding is reflected in the $m$ values recorded in the present work for the three alloys examined (Table II). The 41% Zn alloy with the highest proportion of $\alpha/\beta$ boundaries (42% by volume of $\alpha$) had the highest $m$ value, while the 42% Zn alloy with the highest proportion of $\beta/\beta$ boundaries (32% by volume of $\alpha$) had the lowest $m$ value. However, the ability of boundaries to slide does not appear to be reflected in the ability of the adjoining phases to accommodate the sliding as a comparison of the cavitation behaviour of the 40% Zn and 42% Zn alloys clearly shows. (Figs 2 and 4).

The 40% Zn alloy cavitates rapidly with strain and metallography shows that a relatively high proportion of cavities are associated with $\alpha/\alpha$ boundaries or $\alpha/\alpha/\beta$ junctions, with an approximately equal proportion being located at $\alpha/\beta$ boundaries, or at junctions involving two $\alpha$ and two $\beta$ grains (Fig. 5). The relative ease of cavity nucleation is due to the inability of the predominant phase, $\alpha$, (82% by volume) to make a significant contribution to the accommodation of grain-boundary sliding. Cavity growth and interlinkage leads to failure at relatively small tensile elongations, despite the moderately high $m$ value of the alloy.

While nucleation of cavities during superplastic flow is attributable to grain-boundary sliding, the mechanism of cavity growth, whether by sliding or by diffusional processes, is less certain. The observation that for a constant level of strain the level of cavitation remains approximately constant while the strain rate, and hence the time, is changed by an order of magnitude (Fig. 3), suggests that neither diffusional growth nor diffusional accommodation play a major role in cavitation during superplastic flow in this alloy. This observation is consistent with the findings of Miller and Langdon [11] who recently considered mechanisms of cavity growth in several superplastic alloys, including an essentially single-phase copper alloy [12, 13]. They concluded that although stress-directed vacancy diffusional growth might be important at small cavity sizes, growth to the much larger dimensions, $> 1\,\mu$m, typical of non-coalesced cavities seen in Fig. 4a and b, must occur primarily by plastic deformation. The small drop in the level of cavitation at the highest strain rate examined is due to the deformation involving Stage III of the stress–strain rate curve (Fig. 1). In this region, grain-boundary sliding, which is associated with cavitation, would decrease and there would be an increasing dislocation contribution to the deformation processes.

Previous work on microduplex $\alpha/\beta$ nickel-silvers which contained about 85 vol% of $\alpha$ phase also showed very marked cavitation during superplastic tensile flow, and the level of cavitation for a constant strain was independent of both strain rate and temperature [6].

The 41% Zn alloy shows the highest tensile elongations. These elongations result from an optimum combination of high $m$ value, and hence a high resistance to cavity coalescence, associated with a high proportion of $\alpha/\beta$ boundaries, and a lower level of cavitation relative to the 40% Zn alloy, due to the increased proportion of $\beta$ phase. Metallography showed that the highest proportion of cavities was associated with boundaries involving both $\alpha$ and $\beta$ phases (Fig. 5). It was observed that the level of cavitation in this alloy increased with increasing strain rate (Fig. 3). Similar behaviour has been previously reported for an $\alpha/\beta$ brass [3] and was attributed to the decreasing time available for diffusional accommodation of grain-boundary sliding to occur, mainly via the $\beta$ phase. This would lead to an increasing rate of cavity nucleation with increasing strain rate.

The 42% Zn alloy (68 vol% $\beta$) showed generally higher tensile elongations than the 40% Zn alloy (28 vol% $\beta$), despite its lower $m$ value. This is primarily due to the low level of cavitation in the former alloy, and reflects the ability of the $\beta$ phase to accommodate grain-boundary sliding and hence to inhibit cavity nucleation. It is quite clear from Fig. 4c that cavities do not nucleate readily in this alloy. Despite the high proportion of $\beta/\beta$ boundaries in the alloy, metallography showed that about two-thirds of the relatively few cavities present were associated with boundaries or junctions which involved the $\alpha$ phase (Fig. 5).

The relationship between strain-rate sensitivity,

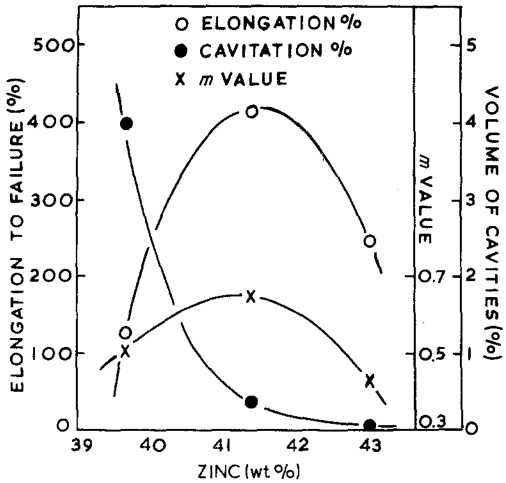


*Figure 6* Relationship between strain rate sensitivity, *m*, elongation to failure, cavitation and alloy composition.

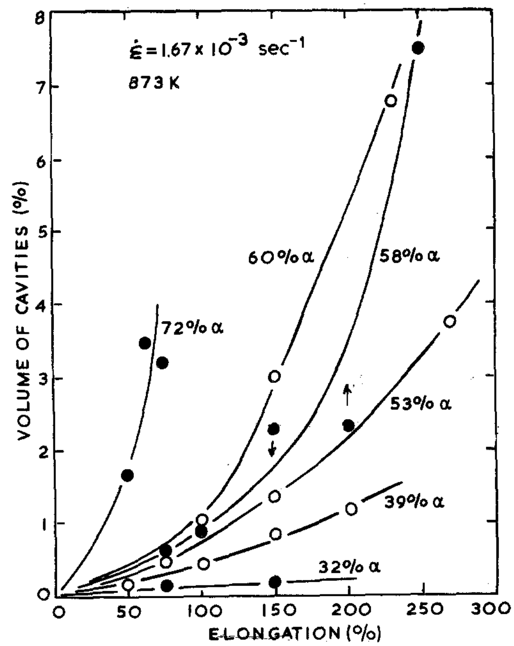


*Figure 7* Volume of cavities as a function of elongation at 873 K for alloys containing various proportions of α phase. Initial strain rate $1.67 \times 10^{-3}\,sec^{-1}$.

*m*, elongation-to-failure (initial strain rate of $8.3 \times 10^{-4}\,sec^{-1}$), cavitation, (75% elongation at an initial strain rate of $8.3 \times 10^{-4}\,sec^{-1}$) and composition is summarized in Fig. 6.

As was noted in Section 3.1, the present study appeared to show some differences in cavitation behaviour compared with earlier measurements on a different series of α/β brasses of compositions nominally similar to the present alloys [7]. During the present work the previous alloys were chemically analysed and the proportions of β phase they contained at 873 K were redetermined (Table I). The variation of void volume with strain for a constant initial strain rate is summarized in Fig. 7 for all alloys and it can be seen that there is an excellent correlation between the volume fraction of β phase present in each alloy and its cavitation behaviour.

Langdon and Taplin [14] have suggested that for cavitation during superplastic flow, small impurity particles would need to be involved in the nucleation event. For a microduplex α/γ stainless steel the important role of Ti (C, N) particles in cavity nucleation has been noted [15], while for a microduplex Pb–Sn alloy of eutectic composition it has been demonstrated that the introduction of hard intermetallic particles induces cavitation during superplastic flow [16]. However, work by Sagat and Taplin [17] on an α/β brass containing iron showed that at low stresses cavities were nucleated at Fe-rich particles, while at higher stresses grain-boundary sites became more important. In the three alloys studied in the present work particles were only occasionally seen, using scanning electron microscopy, to be associated with cavities located in the fracture faces.

## 5. Conclusions

(a) During superplastic tensile straining at 873 K of microduplex α/β brasses containing nominally 40, 41 and 42 wt% Zn, respectively, it was observed that both the strain rate sensitivity index and elongation to failure passed through a maximum when approximately equivolume proportions of α and β phases were present.

(b) Cavitation occurred in the three alloys during superplastic tensile deformation but the level of cavitation for a given strain decreased markedly as the volume fraction of β phase was increased.

(c) Cavitation in the 40% Zn alloy was insensitive to strain rate during superplastic deformation, but increased slowly with increasing strain rate for the 41% Zn alloy. The level of cavitation in the 42% Zn alloy was very low at all strain rates.

(d) The cavitation behaviour reflects the abilities of the phases present to accommodate grain-boundary sliding. In the 40% Zn alloy, which has a high proportion of α phase, accommodation was minimal, and hence cavity nucleation occurred readily. In the 42% Zn alloy with a high proportion of β phase, accommodation was almost complete, and cavity nucleation was minimal.

(e) The insensitivity of the volume fraction of cavities in the 40% Zn alloy to strain rate, and hence to time, is consistent with the view that grain-boundary sliding plays a major role in cavity growth in this alloy.

(f) The high rate of nucleation of cavities, and their subsequent growth and coalescence, is primarily responsible for the relatively low superplastic tensile elongations recorded for the 40% Zn alloy.


## Acknowledgement

One the of the authors (JWDP) would like to thank the Science Research Council for financial support.


## References


1. S. SAGAT, P. BLENKINSOP and D. M. R. TAPLIN, *J. Inst. Met.* **100** (1972) 268.
2. T. CHANDRA, J. J. JONAS and D. M. R. TAPLIN, *J. Mater. Sci.* **13** (1978) 2380.
3. C. W. HUMPHRIES and N. RIDLEY, *ibid.* **13** (1978) 2477.
4. G. L. DUNLOP, E. SHAPIRO, D. M. R. TAPLIN and J. CRANE, *Met. Trans.* **4** (1973) 2039.
5. R. D. SCHELLING and G. H. REYNOLDS, *ibid.* **4** (1973) 2199.
6. D. W. LIVESEY and N. RIDLEY, *ibid.* **9** (1978) 519.
7. N. RIDLEY and D. W. LIVESEY, in "Fracture 77" Vol. 2, edited by D. M. R. Taplin (University of Waterloo Press, Waterloo, Ontario, p. 533.
8. W. A. BACKOFEN, I. R. TURNER and D. H. AVERY, *Trans. ASM* **57** (1964) 980.
9. D. M. R. TAPLIN and T. CHANDRA, *J. Mater. Sci.* **10** (1975) 1642.
10. C. S. SMITHELLS, "Metals Reference Book" (Butterworths, London, 1967) p.658.
11. D. A. MILLER and T. G. LANGDON, *Met. Trans.* **10A** (1979) 1869.
12. S.-A. SHEI and T. G. LANGDON, *J. Mater. Sci.* **13** (1978) 1084.
13. R. G. FLECK and D. M. R. TAPLIN, *Can. Met. Quart.* **11** (1972) 299.
14. T. G. LANGDON and D. M. R. TAPLIN, *Sol. Mech. Archives* **2** (1977) 329.
15. C. I. SMITH, B. NORGATE and N. RIDLEY, *Met. Sci.* **10** (1976) 182.
16. D. W. LIVESEY and N. RIDLEY, *J. Mater. Sci.* **13** (1978) 825.
17. S. SAGAT and D. M. R. TAPLIN, *Acta Met.* **24** (1976) 307.


Received 5 June and accepted 18 July 1980.